INVESTIGATING THE ROLE OF CLPP- AND CLPX-MEDIATED ANTIMICROBIAL RESISTANCE IN *BACILLUS ANTHRACIS*

by

LANG ZOU

Bachelor of Science, 2018
University of Washington
Seattle, Washington

Submitted to the Graduate faculty of the
College of Science and Engineering
Texas Christian University
In partial fulfillment of the requirements
For the degree of

Master of Science

May 2020

ACKNOWLEDGEMENT

I would like to thank my advisor, Dr. Shauna McGillivray, for her help and guidance throughout my project. She has helped me a lot in research, not only about how to do an assay but also about how to setting up experiments and interpret data as an independent scientist. I also appreciate her help in my writing. Dr. McGillivray spent a lot of time helping me with my organization and grammar, which helped me a lot to improve my writing logic. I would also like to thank my committee members, Dr. Giridhar Akkaraju and Dr. Meredith Curtis, for their advice and insight into the direction of my project. I would like to thank Dr. Michael Chumley for helping me with all the fluorescence microscopy.

TABLE OF CONTENTS

LIST OF FIGURES

LIST OF TABLES

Introduction

Bacillus anthracis is a gram-positive, rod-shaped bacterium and the cause of the deadly disease anthrax. It can produce spores and maintain a dormant state that allows it to survive in unfavorable conditions. Spores are the infectious agent and are commonly found in the soil. These spores are highly resistant to dry, high-temperature conditions, so herbivorous animals are potential carriers through feeding behavior. Humans become infected from direct contact, eating infected animal products, or exposure to spores, but spores do not transmit from human to human (Watson et al., 1994). Anthrax fatality rates depend on the route of infection. The most common route is the cutaneous infection, which includes 95% of disease cases. The spores enter the host body through a cut in the skin. Black lesions and swelling form in the skin of the host. If there is no treatment provided, the mortality rate is about 30% (Baillie et al., 2001). Anthrax can also cause gastrointestinal disease through ingestion, which has a 25% to 60% fatality rate (Baillie et al., 2001). Inhalational anthrax, with a 95% fatality rate and the highest fatality among the three types of anthrax, occurs when spores are inhaled into the body. A large amount of spores must be inhaled into the lungs to cause infection, so this type of anthrax is rare (Hart et al., 2002). After bacteria infect the alveoli in the lung, alveolar macrophages containing spores enter the lymph nodes nearby, where the endospores germinate into mature bacteria to kill host cells. These mature bacteria release toxins, which can inhibit the initiation of an immune response after they enter the lymph nodes. The bacteria can then move to other tissues through the bloodstream resulting in the high mortality rate (Hart et al., 2002; Dixon et al., 1999). Due to its deadly nature, *B. anthracis* has been used as a biological weapon, first during WWI, and most recently during

the 2001 bioterrorism attacks which left five dead and seventeen injured after exposure to letters containing spores (Harris et al., 1994; Jernigan et al., 2002).

The fully virulent strain of *B. anthracis* contains chromosomal DNA, which encodes about 5000 genes, and two large plasmids, *p*XO1 and *p*XO2. The *p*XO1 plasmid encodes two toxins, lethal toxin and edema toxin. These toxins enter the cell through endocytosis. The process starts when the protective antigen (PA), a component of both toxins, binds to an anthrax toxin receptor on the cell surface (Agrawal et al., 2004). The formation of this PA-heptamer helps translocate the edema factor (EF) and lethal factor (LF) into the cell cytoplasm. Once in the cytosol, EF and LF carry out a damage-inducing process through different pathways. EF forms a complex with calmodulin (CaM) to greatly increase the cAMP level in the cell, leading to an imbalanced intracellular signaling pathway and impaired immune cell function (Singh et al., 1989). Then the edema toxin induces the cell lysis of macrophages to suppress the host immune system. The lethal toxin also helps the bacteria to evade the immune system by killing macrophages but using a different mechanism from EF. Once inside the cell, the LF cleaves the mitogen activated protein kinase (MAPK). The kinase cannot bind to the original substrate, thus the mitogen activated protein kinase (MAPK) signaling pathway is inhibited (Agrawal et al., 2004). The disruption of the MAPK pathway causes the deficiency in proliferation, survival, and inflammation (Singh et al., 1989). In addition to the virulence conferred by the *p*XO1 plasmid, the *p*XO2 plasmid encodes genes that synthesize the capsule, which can protect the bacteria from phagocytosis (Dixon et al., 1999). Many studies have focused on toxins and capsule and their importance in virulence while the role of the chromosomal genes is less well-studied. In 2003, the entire genome of *B. anthracis* was sequenced for the first time, and the study found some chromosomally encoded genes that may contribute to pathogenicity based on sequence

homology with known virulence factors in other bacterial pathogens (Read et al., 2003). Therefore, our lab has focused on the discovery of potential chromosomal virulence factors of *B. anthracis*.

Previous research in our lab resulted in the generation of a random chromosomal mutant library of the Sterne strain of *B. anthracis* through transposon mutagenesis (McGillivray et al., 2009). The Sterne strain lacks the *p*XO2 plasmid, and is unable to cause disease in humans due to the absence of capsule. Transposon mutants were screened for loss of virulence-associated phenotypes, including lack of hemolytic activity. This strategy identified a mutation in a gene called *clpX* (McGillivray et al., 2009). Deletion of *clpX*, even in a fully virulent strain of *B. anthracis*, results in complete loss of virulence for *B. anthracis* in mammalian models of infection (McGillivray et al., 2009). ClpX functions as a regulatory ATPase, and together with caseinolytic peptidase (ClpP) forms the ClpXP protease (Frees et al., 2007; Baker et al., 2012). ClpX recognizes proteins, such as metabolic enzymes, stress response proteins, regulatory proteins, and damaged or misfolded proteins. ClpX uses the energy produced by ATP hydrolysis to unfold the tertiary structure (Frees et al., 2007; Baker et al., 2012). It then feeds them into a proteolytic core created by ClpP, which degrades them. Because ClpXP controls the degradation of multiple proteins in the cell, it functions as a global regulator and loss of the protease can have multiple effects on the cell. Orthologs of ClpXP are shared in many bacterial species with similar functions in cellular stress regulation (Frees et al., 2007).

In *B. anthracis*, in addition to playing a key role in overall virulence, ClpX is also necessary for resistance to a number of antimicrobials including antibiotics such as penicillin, daptomycin and nisin as well as the human antimicrobial peptide, LL-37 (McGillivray et al., 2009;

McGillivray et al., 2012). One thing all of these antimicrobials have in common is that they either directly target the cell wall (penicillin, nisin) (Nikolaidis et al., 2014) or interact with the cell wall on their way to the cell membrane (daptomycin, LL-37 and nisin) (Muthaiyan et al., 2008; Thwaite et al., 2006). Because of these specific targets, later research focused on determining whether there are morphological changes to the bacterial cell wall in the Δ*clpX* strain. A study by a previous graduate student in our lab examined the *B. anthracis* cell wall using transmission electron microscopy and found a significant decrease in the cell wall thickness in the Δ*clpX* strain (Evans, unpublished data). With a thinner cell wall, the bacteria might have a reduced ability to block antimicrobial entry, resulting in increased cell wall-targeting antibiotic susceptibility (Hanaki et al., 1998; Mishra et al., 2011). In addition to having a thinner cell wall, there were unexpected cell division defects in Δ*clpX* (Evans, unpublished data). Therefore, loss of *clpX* in *B. anthracis* contributes to both reduced virulence and increased antimicrobial susceptibility and leads to morphological changes in the cell wall that may, at least partially, account for these phenotypes.

Our research has shown that ClpX is important for antibiotic resistance; however, ClpX can function both independently as a chaperone (Wawrzynow et al., 1995), or together with ClpP to form the ClpXP protease (Baker et al., 2012). Therefore, it is not yet clear if ClpX mediates antibiotic resistance independently as a chaperone protein or together with ClpP as a part of the ClpXP protease. A previous study in our lab tested the effects of a ClpXP protease inhibitor, F2, and found that F2 increased the susceptibility to antimicrobial peptides and penicillin in *B. anthracis* in a manner similar to that seen with the loss of the *clpX* gene (McGillivray et al., 2012). Based on this, we hypothesize that ClpX-mediated antibiotic resistance is dependent on the formation of the ClpXP protease. To test this, we first made a substitution mutation at the

ClpP-ClpX interaction site that prevents protease formation to determine whether this mutated strain can mediate antibiotic resistance. Next we specifically disrupted ClpP in *B. anthracis*. Interestingly, *B. anthracis* has two ClpP subunits, which is uncommon in gram-positive bacteria (McGillivray et al., 2012). These are named ClpP#1, and ClpP#2 based on their initial characterization in the related species, *Bacillus thuringiensis* (Fedhila et al., 2002). There are at least two other bacterial species, the acid-fast *Mycobacterium tuberculosis* (Rahy et al., 2012) and gram-negative *Pseudomonas aeruginosa* (Hall et al., 2017), that also contain two *clpP* genes, but they are not closely related to *B. anthracis*. We genetically disrupted both ClpP#1 and ClpP#2 individually to determine how each are contributing to antibiotic resistance in *B. anthracis* Sterne.

Methods

Alignment

Protein sequence of *S. aureus* ClpX and *B. anthracis* ClpX were extracted from the Uniprot database (http://www.uniprot.org/) and aligned using CLUSTALW (https://npsa-prabi.ibcp.fr/cgi-bin/npsa_automat.pl?page=npsa_clustalw.html). Protein sequences of *M. tuberculosis* ClpP#1 and ClpP#2, *P. aeruginosa* ClpP#1 and ClpP#2, *B. anthracis* ClpP#1 and ClpP#2 were extracted from the Uniprot database (http://www.uniprot.org/) and aligned using BLASTP (https://blast.ncbi.nlm.nih.gov/Blast.cgi).

Bacterial strains and growth conditions

The parental *B. anthracis* strain used in this study is *B. anthracis* Sterne ($pXO1^+$, $pXO2^-$). *B. anthracis* Δ*clpX* was previously described (McGillivray et al. 2009). The wild-type parental *B. anthracis* Sterne carrying the empty inducible plasmid *p*UTE657, the isogenic Δ*clpX* mutant

containing empty *p*UTE657 and the Δ*clpX* mutant complemented with the wild-type *clpX* gene in *p*UTE657 (*pclpX*) were made previously (Claunch et al., 2018). The Δ*clpX* +*pclpX*^{I265E} mutant, the two *clpP* insertional mutants and the *clpP#1* and *clpP#2* complemented strains were constructed during this study and are described below. *B. anthracis* cultures were grown in brain heart infusion (BHI) (Criterion) at 37° C shaking under aerobic conditions. 0.1 mM isopropyl β-d-1-thiogalactopyranoside (IPTG) was added when inducing the expression plasmid.

Construction of *clpX*^{I265E} plasmid

A substitution mutation at position 265 from isoleucine (ATT) to glutamic acid (GAA) of the *B. anthracis clpX* gene was made in the wild-type *clpX* expression plasmid that was previously constructed (Claunch et al., 2018) to yield the *clpX*^{I265E} plasmid. To do this, site-directed mutagenesis (NEB) was performed using the primers Ba_ClpX I265E_Fwd (5'- TGA AAA GGT AGA GGG ATT TGG TTC TGA GAA G -3') and Ba_ClpX 1265E Rev (5'- CCA AGA CGG CGT TTA ATA ATT G -3') following manufacturer's instructions. Following mutagenesis, the plasmid was sequenced to confirm that the mutagenesis was successful.

Construction of *B. anthracis clpP#1* and *clpP#2* insertional mutants

Approximately 300bp of DNA within the middle of the *clpP#1* gene was amplified with primers ClpP#1 IM-2 Fwd-HindIII (5'- ATG CAA GCT TAA CGC GCT TAC GAT ATT TAC TCT C -3') and ClpP#1 IM-2 Rev-BamHI (5'- GCA TGG ATC CGC TTC ACT GTT TGG AAG TGC -3'). Approximately 270bp of DNA within the *clpP#2* gene was amplified with primers ClpP#2 IM-2 Fwd-HindIII (5'- ATG CAA GCT TAG ACC GTA TTG TTA TTA TCG GTT CAG A -3') and ClpP#2 IM-2 Rev-BamHI (5'- GCA TGG ATC CCA CTA TTT GGG AGT GCA AAT CGT -3'). The resulting amplicon was sub-cloned into the temperature-sensitive plasmid

*p*HY304 using HindIII and BamHI restriction endonucleases and transformed into electrocompetent MC1061F *Escherichia coli* cells (Lucigen) first and then into the methylation deficient *E. coli* strain GM2163. After purification from GM2163 cells, the mutagenesis plasmid was transformed into *B. anthracis* Sterne, and transformants were confirmed using primers pHY3065 Fwd (5' - ACG ACT CAC TAT AGG GCG AAT TGG - 3') and pHY3260 Rev (5' - GCG GAT AAC AAT TTC ACA CAG G - 3'). *B. anthracis* Sterne with the mutagenesis plasmid (*p*HY304 *clpP#1 IM* or *p*HY304 *clpP#2 IM*) was grown overnight in BHI with 5 μg/ml erythromycin at 30°C, and then incubated at 37°C for at least 8 hours shaking under erythromycin selection to force plasmid integration. The *B. anthracis clpP#1* insertional mutant was confirmed using primers pHY3065 Fwd (5' - ACG ACT CAC TAT AGG GCG AAT TGG - 3') and Ba ClpP1 EV-2 Rev SphI (5' - TGC AGC ATG CGA TTC TAA ACG AGC CGC TTC CG - 3'), and the *B. anthracis clpP#2* insertional mutant was confirmed using primers pHY3065 Fwd (5' - ACG ACT CAC TAT AGG GCG AAT TGG - 3') and Ba ClpP2 EV Rev SphI (5' - TGC AGC ATG CAC TTT ACT CTC TAG CCT GCT TTC TG - 3').

Construction of *B. anthracis clpP#1* and *clpP#2* double knockout plasmid

Approximately 270bp of DNA within the middle of *clpP#2* was amplified with primers ClpP#2 IM-2 Fwd-NotI (5'- ATG CGC GGC CGC AGA CCG TAT TGT TAT TAT CGG TTC AGA - 3') and ClpP#2 IM-2 Rev-BamHI (5'- GCA TGG ATC CCA CTA TTT GGG AGT GCA AAT CGT -3'). The resulting amplicon was sub-cloned into a different temperature-sensitive plasmid *p*HY304-Kan, which contains an additional antibiotic resistance gene for kanamycin, using NotI and BamHI restriction endonucleases and transformed into MC1061F competent cells (Lucigen) first and then into methylation deficient cells, GM2163.

Construction of *clpP#1* and *clpP#2* expression plasmids

The expression plasmid *pclpP#1* was constructed by amplifying the complete *clpP#1* sequence using primers Ba ClpP#1 EV-2 Fwd SalI (5'- ATG CGT CGA CGG TTT CGT TTG ACC TTT ATT GAC -3') and Ba ClpP#1 EV-2 Rev SphI (5'- TGC AGC ATG CGA TTC TAA ACG AGC CGC TTC CG -3'). The expression plasmid *pclpP#2* was constructed by amplifying the complete *clpP#2* sequence using primers Ba ClpP#2 EV Fwd SalI (5'- ATG CGT CGA CTG CTT TGC GTT GCA TAA CAA TTA TTG -3') and Ba ClpP#2 EV Rev SphI (5'- TGC AGC ATG CAC TTT ACT CTC TAG CCT GCT TTC TG -3'). The amplicons were then sub-cloned into *p*UTE657 [3] using SalI and SphI restriction endonucleases (NEB) for both *clpP* sequences and transformed into MC1061F (Lucigen) competent cells first and then into methylation deficient cells, GM2163. The expression plasmids were then transformed into the *B. anthracis* Δ*clpP#1* or Δ*clpP#2* insertional mutants for complementation, and transformants were grown at 37 °C under spectinomycin selection. As controls for the plasmid, the *p*UTE657 empty vector was transformed into *B. anthracis* Δ*clpP#1* or Δ*clpP#2* insertional mutants, and transformants were grow at 37°C under spectinomycin selection as well. The complemented strains for both *B. anthracis clpP#1* and *clpP#2* insertional mutants were confirmed using primers pUTE657 Fwd (5' - GAA CGT TGC TCG AGG GTA AAT G - 3') and pUTE657 Rev (5' - GGT ACG TAC GAT CTT TCA GCC - 3'). The correct sequence of the *clpP#1* and *clpP#2* genes in *p*UTE657 were confirmed by sequencing.

Minimum inhibitory concentration assays

Overnight cultures were diluted 1: 20 and grown to early log phase at an optical density (OD) of 0.4 at 600 nm wavelength. Assays using nisin, vancomycin, penicillin, ciprofloxacin, erythromycin, tetracycline and chloramphenicol (all Sigma) were performed in BHI (Hardy

Diagnostics) and incubated at indicated concentrations. Assays using LL-37 (Anaspec) were performed in Roswell Park Memorial Institute 1640 medium (RPMI; Corning) supplemented with 5% Luria–Bertani (LB) medium (Hardy Diagnostics), and incubated at indicated concentrations. Assays using daptomycin (Cubist pharmaceuticals) were grown in Mueller–Hinton Broth II supplemented with 50 μg/ml calcium (CA-MHB), and incubated at indicated concentrations. For testing LL-37 and daptomycin, cultures were pelleted, washed and re-suspended in an equivalent volume of RPMI+ 5% LB for LL-37 and CA-MHB for daptomycin. Assays were performed in 96-well plates, which were incubated overnight for 20 hours at 37°C under static conditions except for the daptomycin assays, which were incubated in 96 round-well plates overnight for 20 hours at 37°C shaking. Following incubation, the OD of each well was measured at 600 nm wavelength. 0.1 mM IPTG was included in the overnight culture, log phase culture and assay media for assays testing strains with the expression plasmid in order to induce expression.

Hydrophobicity assay

Wild-type parental *B. anthracis* and the isogenic Δ*clpX* mutant *B. anthracis* were grown overnight at 37°C in BHI media. Cultures were harvested and washed twice with PBS and resuspended in 200 μl PBS. The concentrated bacteria were then added to 3 ml PBS to reach an OD of 0.5 at 600 nm wavelength (A0). 1 ml of the hydrophobic hydrocarbon, n-hexadecane (Sigma-Aldrich) was added to each tube containing the 3 ml of bacteria. After vigorous vortexing, phases were allowed to separate for 30 min at room temperature and the OD600 nm of the lower aqueous phase was measured (A1). The percentage of hydrophobicity was calculated as follows: hydrophobicity (%) = [1−(A1/A0)] × 100. This was normalized to wild-type Sterne *B.*

anthracis (WT=1) by using the percentage hydrophobicity calculated for each mutant strain divided by the hydrophobicity percentage of the wild-type Sterne and this relative hydrophobicity is presented in the graph.

Buoyancy assay

The concentration gradient of Percoll solutions was created by layering 1 ml each of 70%, 60% and 50% solutions (50% is the top layer) in glass test tubes. Wild-type parental *B. anthracis* Sterne (WT) and the isogenic Δ*clpX* mutant containing empty inducible plasmid (*p*UTE657) and Δ*clpX* complemented with either *clpX* (*pclpX*) or I265E point mutation ($pclpX^{I265E}$) were grown at 37 °C overnight in BHI supplemented with 0.1 mM IPTG for plasmid expression. 1 ml of each overnight culture was added to the top of the Percoll gradient. After centrifuging at 620 rpm at 4°C for 1 hour using the Allegra™ 6R centrifuge (Beckman Coulter), the distance from the bottom of the test tube to the lowest migrated band was measured.

Growth curve

Overnight cultures of wild-type *B. anthracis* Sterne, Δ*clpX,* Δ*clpP#1* insertional mutant and Δ*clpP#2* insertional mutant were diluted 1:20 and grown to early log phase at an optical density of 0.4 at 600 nm wavelength. Log phase cultures were then diluted 1:100 in the indicated media: Brain-Heart Infusion (BHI), RPMI-5% LB, or CA-MHB medium. Growth was monitored over an 8-hour period by measuring the optical density of cultures in 1-hour increments.

***Galleria mellonella* assay**

G. mellonella were obtained from Rainbow Mealworms (www.rainbowmealworms.net). Larvae weighing 190-200mg were placed into groups of twelve for injection. Larvae were kept at 4°C

prior to injection to reduce movement. Wild-type *B. anthracis* Sterne, isogenic Δ*clpX* mutant, insertional mutant Δ*clpP*#1 and insertional mutant Δ*clpP#2* strains were grown overnight, diluted 1:20, and grown to early log phase (OD 0.4) in BHI. Once OD 0.4 was reached, bacteria were washed and suspended in PBS at a 1:2 dilution. Larvae were injected with 10 µl of 1:2 diluted bacteria (approximately $8x10^4$ cfu/larvae) and starting amounts were confirmed through colony counts of original cultures. After injection, larvae were observed at room temperature to ensure they recovered from injection and were transferred to an incubator at 37°C. Dead larvae were counted at 24, 48, and 72-hours post injection.

Scanning electron microscopy

Bacterial cultures of wild-type *B. anthracis* Sterne and Δ*clpX* were grown overnight in BHI, washed once in PBS and resuspended and fixed in 2.5% glutaraldehyde for 1 hour at room temperature. The samples were then dehydrated with a series of 10-minute alcohol incubations at the following concentrations (in order): 30%, 50%, 70%, 85%, 90%, and 100%. The incubation with 100% alcohol was performed twice. Next, samples were incubated with hexamethyldisilazane overnight with the tube lid open to allow excess liquid to evaporate. The dry pellet was crushed and transferred to a metal pedestal and sputter coated with 8 nm of gold. Images were taken at 2kV with a JEOL JSM-6100 Scanning Microscope.

Fluorescence microscopy

Wild-type parental *B. anthracis* and the isogenic Δ*clpX* mutant *B. anthracis* were grown overnight at 37°C in BHI or RPMI+5% LB media. Cultures were harvested and washed twice with PBS and resuspended in 250 µl. Stationary phase bacteria were incubated with 2 µg/ml of

FM 4-64 (ThermoFisher) in the dark for one hour at 37°C under static condition. Then 5 µl of each resuspended bacteria were added to slide with 1 µl of Fluoromount-G (SouthernBiotech), and let it dry at room temperature. All slides (premiere) and cover glasses (Fisherbrand) were poly-lysine coated (George, 2008). The studies were performed using a Zeiss LSM 710 laser-scanning confocal microscope (Thornwood, NY) and images were analyzed using Zeiss Zen software.

Results

The inhibition of ClpXP protease formation

In order to determine whether ClpX-mediated antimicrobial resistance (McGillivray et al., 2012) and morphological changes (Evans, unpublished data) are ClpP dependent, we inhibited the ClpXP protease formation by using the strategy recently described in *S. aureus* (Stahlhut et al., 2017). In *S. aureus*, a substitution mutation was made in ClpX at position 265 to change isoleucine to glutamic acid. This prevents ClpX from interacting with ClpP and forming the ClpXP protease (Stahlhut et al., 2017). The protein sequence alignment using CLUSTALW showed that *B. anthracis* and *S. aureus* have overall 86.69% identical or strongly similar amino acid sequence,

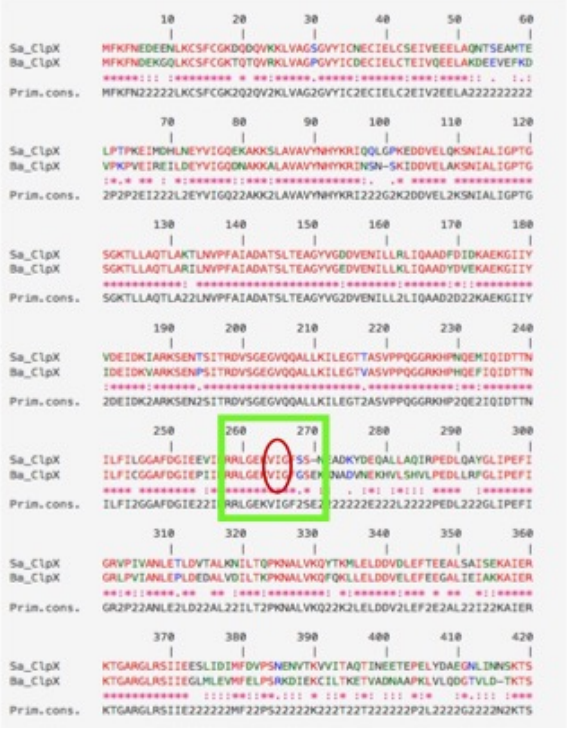

Figure 1. Protein alignment of ClpX from *B. anthracis* and *S. aureus*.
The amino acid sequences of ClpX in *S. aureus* and *B. anthracis* were aligned using CLUSTALW. The green box represents where ClpX and ClpP interact to form the ClpXP protease. The isoleucine (I) at position 265 (red circle) is essential for protease formation.

and the amino acids at the ClpX-ClpP interaction site (green box, Fig. 1) are mostly identical. Based on these high levels of similarity, we reasoned that disrupting the same amino acid in ClpX in *B. anthracis* Sterne would also prevent ClpXP formation. Using site directed mutagenesis an undergraduate in our lab, Quinn Losefsky, made a substitution mutation at position 265 from isoleucine (ATT) to glutamic acid (GAA) in the *clpX* expression plasmid to create the plasmid $pclpX^{I265E}$. After confirming the mutagenesis by sequencing, Δ*clpX B. anthracis* were transformed with $pclpX^{I265E}$. Four different strains of *B. anthracis* were then generated: wild-type *B. anthracis* containing the empty expression plasmid *p*UTE657 (WT+ *p*UTE657), the isogenic *clpX* knockout (Δ*clpX* +*p*UTE657), the *clpX* knockout strain complemented with wild-type *clpX* (Δ*clpX* +*pclpX*), and the *clpX* knockout strain complemented with the mutated ClpX that is unable to interact with ClpP (Δ*clpX* +$pclpX^{I265E}$) strain (Fig. 2a).

Preventing formation of the ClpXP protease in *B. anthracis* increases the susceptibility to cell envelope-targeting antibiotics

To determine the effects of losing the protease function of ClpX on antimicrobial susceptibility, we performed the minimum inhibitory concentration (MIC) assay on our 4 bacterial strains using two antimicrobial peptides and three antibiotics. Penicillin and vancomycin, which target the cell wall, and nisin, daptomycin and LL-37 which target the cell membrane (Fig. 2a).

As expected, there was a significant difference in growth between the wild-type *B. anthracis* and Δ*clpX* strain treated by both antimicrobial peptides, nisin (200 μg/ml) and LL-37 (2 μM), and all three antibiotics, penicillin (2.5 μg/ml), vancomycin (6 μg/ml) and daptomycin (2 μg/ml). This growth defect was rescued in the strain complemented with wild-type *clpX* (Fig. 2b-f). However, when we complemented with $clpX^{I265E}$, the levels of growth were the same as

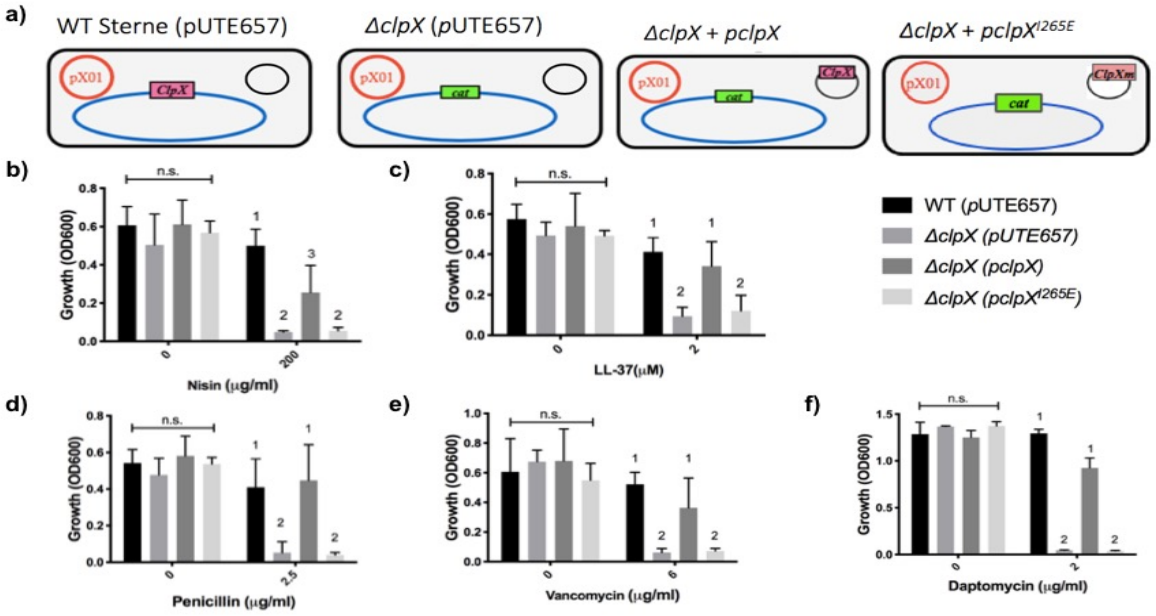

Figure 2. The formation of ClpXP protease is necessary for antimicrobial resistance in *B. anthracis*.

a) Schematic of the 4 bacterial strains: wild-type parental *B. anthracis* Sterne carrying the empty inducible plasmid *p*UTE657 (black circle) used for all complementation assays, the isogenic Δ*clpX* mutant containing empty *p*UTE657, the Δ*clpX* mutant complemented with the wild-type *clpX* gene in *p*UTE657 (*pclpX*) and the Δ*clpX* mutant complemented with the *clpX* gene containing a mutated interaction site at position 265 from isoleucine to glutamic acid ($pclpX^{I265E}$). b-f) Growth of wild-type parental *B. anthracis* Sterne (WT), Δ*clpX* mutant containing empty inducible plasmid (*p*UTE657), and Δ*clpX* complemented with either the wild-type *clpX* gene (*pclpX*) or the *clpX* gene containing the I265E point mutation ($pclpX^{I265E}$) in media containing either (b) nisin, (c) LL-37 (d) penicillin, (e) vancomycin or f) daptomycin at the indicated concentrations. Data is presented as mean+/- SD and assays were repeated at least 3 independent times. Different numbers represent statistically significant differences between groups ($P<0.05$) and n.s. means no statistical difference between groups as determined by one-way ANOVA followed by Tukey–Kramer post hoc analysis.

Δ*clpX* in all antimicrobials tested. Therefore, we conclude that ClpX-mediated antibiotic resistance is dependent upon the interaction with ClpP through the ClpXP protease rather than through ClpX- independent mechanisms.

Preventing the formation of ClpXP protease in *B. anthracis* alters the cell density

Since all the antimicrobial peptides and antibiotics we tested target the cell envelope, which comprises the cell membrane and cell wall, we next wanted to know whether disrupting

the function of the ClpXP protease alters the physical characteristics of the cell envelope. A previous graduate student in the lab found that Δ*clpX* had decreased cell wall thickness using transmission electron microscopy (Evans, unpublished data). We used an alternative strategy called a buoyancy assay to measure the difference in cell density among our strains. The cell wall is a major determinant of cell density and therefore this is an indirect way assess cell wall thickness. Cell density is represented by measuring how far the bacteria are able to move through an increasing density gradient. We made the density gradient by using different concentrations of Percoll solution, and added the bacteria solution on the very top (Fig. 3a).

Each test tube with bacteria strain was incubated at 4°C, and centrifuged for one hour to measure the ability of bacteria to penetrate through the density gradient. The different bacterial strains traveled different distances in the density gradient as indicated by the red arrows (Fig. 3b).

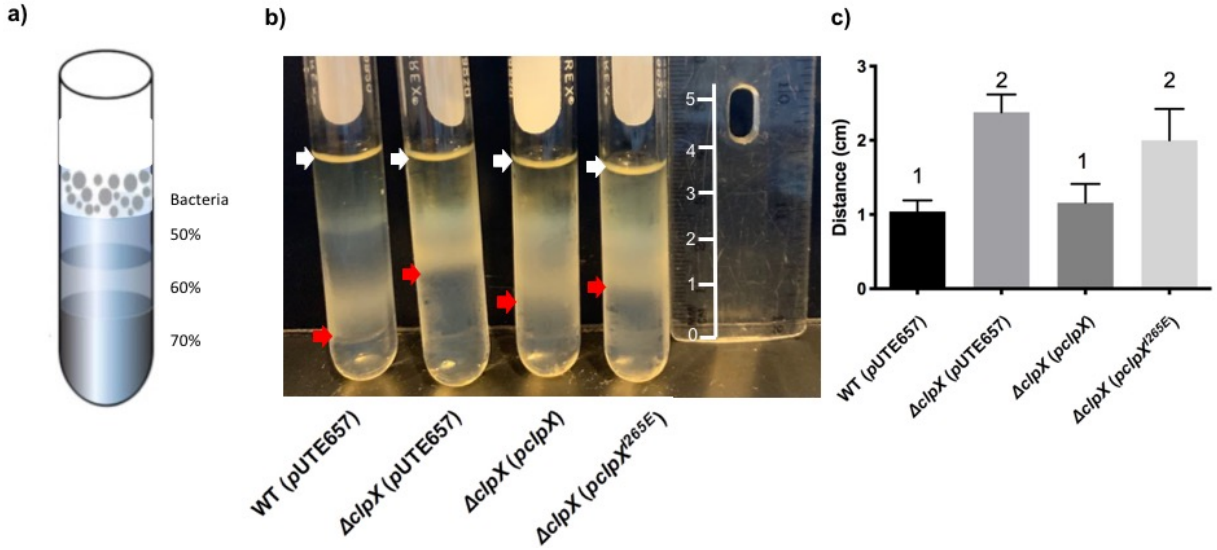

Figure 3. The formation of ClpXP protease is necessary to maintain cell density in *B. anthracis*.
a) Schematic of the density gradient where Percoll solutions at the indicated concentrations were layered on top of one another with a layer of overnight bacterial culture added at the top before centrifugation. b) Representative image of the distance the different bacterial strains were able to travel through the gradient. White arrows represent the starting point of the bacteria; red arrows, the position of bacteria after centrifugation and travel through the gradient. c) Graph represents the mean distance from the bottom of the tube for each strain +/- SD of four independent experiments. Different numbers represent statistically significant differences between groups ($P<0.05$) as determined by one-way ANOVA followed by Tukey–Kramer post hoc analysis.

The layers of wild-type *B. anthracis* and complemented strains were closer to the bottom of the tube, which means they moved further through the density gradient. Data from multiple assays were compiled (Fig. 3c) and show that the Δ*clpX* and the Δ*clpX*+ $pclpX^{I265E}$ mutants did not migrate as far as the wild-type or the complemented strains. We conclude that the loss of *clpX* and the inability to form the ClpXP protease decreased the cell density of the Sterne *B. anthracis*.

Preventing the formation of ClpXP protease in *B. anthracis* leads to an increase in cell surface hydrophobicity

Besides cell density, another component of the cell envelope we tested is cell surface hydrophobicity. A previous study on *S. aureus* found that an antibiotic-resistant *S. aureus* strain showed higher surface hydrophobicity than the wild-type, suggesting a correlation between antibiotic resistance and cell surface (Lather et al., 2016). The resistant strain tends to have higher surface hydrophobicity compared to the wild-type. We used a hydrophobic solution, hexadecane to determine the adhesion ability of wild-type *B. anthracis* +*p*UTE657, Δ*clpX* +*p*UTE657, Δ*clpX* +*clpX* complement, and Δ*clpX* +$pclpX^{I265E}$ strains. Absorbance of an overnight bacterial culture was measured and then the culture was mixed vigorously with hexadecane, incubated under static conditions and absorbance of the aqueous layer was measured again. The difference in absorbance before and after incubation represents the ability of the bacterial strain to adhere to the hexadecane. A larger decrease in absorbance indicates a higher level of hydrophobicity. The relative hydrophobicity of each strain was determined by calculating the percentage change in absorbance and then normalizing to the wild-type value, which was set at 1. The Δ*clpX* +*p*UTE657 and the Δ*clpX* +$pclpX^{I265E}$ mutants showed significantly larger change in absorbance after incubation compared to either wild-type *B. anthracis* +*p*UTE657 or Δ*clpX* +*clpX* complement strain (Fig. 4). This suggests that their cell

surfaces are more hydrophobic compared to that in the wild-type and the Δ*clpX* +*pclpX* complemented strain.

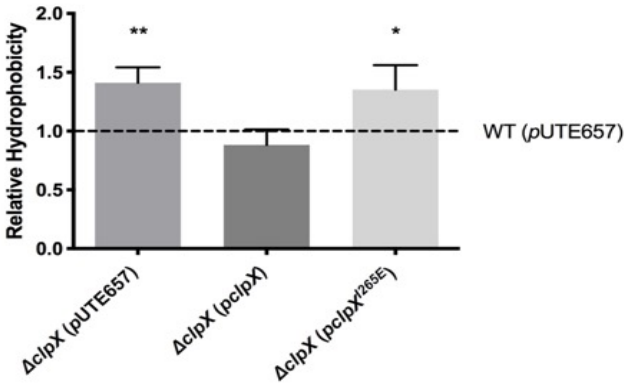

Figure 4. Wild-type and Δ*clpX B. anthracis* exhibit differences in cell surface hydrophobicity. Relative hydrophobicity of the wild-type parental *B. anthracis* Sterne (WT) and the isogenic Δ*clpX* mutant containing empty inducible plasmid (*p*UTE657) and Δ*clpX* complemented with either wild-type *clpX* (*p*clpX) or the I265E point mutation (*pclpX*^{I265E}) as measured to adherence to hexadecane. Data is presented as mean+/- SD and assays were repeated 4 independent times. Statistically significant differences from wild-type are represented by *P<0.05, **P<0.01, as determined by a one-sample t-test.

Examination of Δ*clpX*+*pclpX*^{I265E} cellular morphology using fluorescence microscopy and scanning electron microscopy

To further observe the cell division defects in Δ*clpX* (Evans, unpublished data), we used fluorescence microscopy and the membrane-staining dye FM4-64 as a way to visualize division sites. However, the resolution of the confocal microscope and the inefficient staining made it hard to clearly see any division sites in the bacterial cells, much less see any differences between wild-type *B. anthracis* and Δ*clpX*. We then used the scanning electron microscopy to look at division sites. We saw mostly normal cells in wild-type and some mini-cell formation in Δ*clpX*. Mini-cells are small

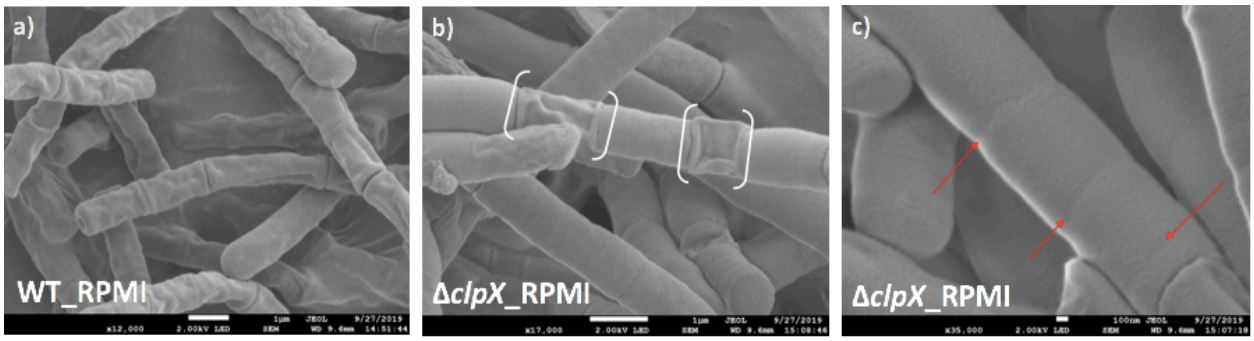

Figure 5. Scanning electron microscopy shows some difference in cell division sites. Stationary phase of wild-type *B. anthracis* Sterne (a) and *ΔclpX B. anthracis* (b-c) cultures grown in RPMI +5% LB. Sections were visualized at 2kV at 17,000x magnification in (a-b), (c) was visualized at 35,000x magnification. White brackets (b) showed representative mini-cell in *ΔclpX B. anthracis*. Red arrows represent the potential additional cell division sites.

bacterial cells produced through too frequent cell divisions (Fig. 5a-b, brackets). This could also be seen in Fig. 5c as increased septum formation (red arrows). Therefore, our results with SEM support the earlier observations made using TEM (Evans, unpublished data) although the divisions sites cannot be seen as clearly when only visualizing the surface of SEM.

Construction of ClpP insertional mutant in *B. anthracis*

Since we have found that the ClpX-mediated antibiotic resistance and morphological changes are dependent on the ClpP subunit, the second objective of the project is to determine the role of each ClpP subunit in *B. anthracis*. The two ClpP subunits in *B. anthracis* are very similar to each other, with 66.32% of the amino acid sequences identical and 88.08% of the amino acid sequence identical plus strongly similar (Table. 1). It is rare for bacterial species to have two ClpP subunits (McGillivray et al., 2012), however the unrelated species, *Mycobacterium tuberculosis,* an acid-fast bacterium, and *Pseudomonas aeruginosa*, a gram-

a)

% Identical amino acids	*B.anthracis* ClpP#1	*B.anthracis* ClpP#2	*M.tuberculosis* ClpP#1	*M.tuberculosis* ClpP#2	*P.aeruginosa* ClpP#1	*P.aeruginosa* ClpP#2
B.anthracis ClpP#1		66.32%	46.00%	44.86%	62.91%	35.64%
B.anthracis ClpP#2	66.32%		46.50%	39.25%	53.99%	32.18%

b)

% Identical+ Strongly similar amino acids	*B.anthracis* ClpP#1	*B.anthracis* ClpP#2	*M.tuberculosis* ClpP#1	*M.tuberculosis* ClpP#2	*P.aeruginosa* ClpP#1	*P.aeruginosa* ClpP#2
B.anthracis ClpP#1		88.08%	73.00%	67.29%	79.34%	62.87%
B.anthracis ClpP#2	88.08%		71.5%	65.89%	73.71%	57.92%

Table 1. Sequence homology of ClpP subunits.
Multiple protein sequence alignment of ClpP subunits from *B.anthracis, M. tuberculosis* and *P.aeruginosa* were performed using the CLUSTALW online program. Percent identical amino acid sequence (a) and percent identical and strongly similar amino acid sequence (b) are shown.

negative bacterium, also have two ClpP sequences. The two ClpP subunits are highly similar in all three bacteria, which suggests that they may have a conserved function among the species.

To investigate the role of *clpPs* in *B. anthracis,* we individually disrupted each of the *clpP* genes in *B. anthracis* Sterne through insertional mutagenesis. We first amplified a 300 bp-PCR fragment from the middle of the *clpP#1* gene and sub-cloned it into the temperature sensitive plasmid, *p*HY304 using restriction enzymes that were engineered onto the ends of the PCR fragment. The constructed vector was then transformed into wild-type *B. anthracis* where it integrated into the middle of the *clpP#1* gene through homologous recombination (Fig. 6a). The insertional mutant for Δ*clpP#2* was created in a similar way (Fig. 7a). To confirm the successful recombination of the plasmid into the *B. anthracis* genome, PCR was used to amplify the recombined DNA by using a *p*HY304 specific primer and a primer downstream of the insertional site. We expect to have no bands for wild-type Sterne *B. anthracis*; however, there was a band shown for the wild-type *B. anthracis* (Fig. 7b) at the incorrect size, which could be non-specific priming. As expected, a band about 450bp was seen for the both Δ*clpP#1* and Δ*clpP#2* insertional mutants (Fig. 6b, 7b). The creation of these two new mutant strains resulted in a total of 4 *B. anthracis* Sterne strains: wild-type *B. anthracis*, the isogenic Δ*clpX* mutant, and the Δ*clpP#1* and Δ*clpP#2* insertional mutants (Fig. 9a).

The insertional mutation in either Δ*clpP#1* or Δ*clpP#2* increases the susceptibility to cell envelope-targeting antibiotics

To make sure the media we used for the MIC assays had no effect on bacterial growth, we grew wild-type *B. anthracis* Sterne, Δ*clpX,* Δ*clpP#1* and Δ*clpP#2* insertional mutants in BHI (Fig. 8a), RPMI+5%LB (Fig. 8b) and CA-MHB (Fig. 8c) and measured optical density every

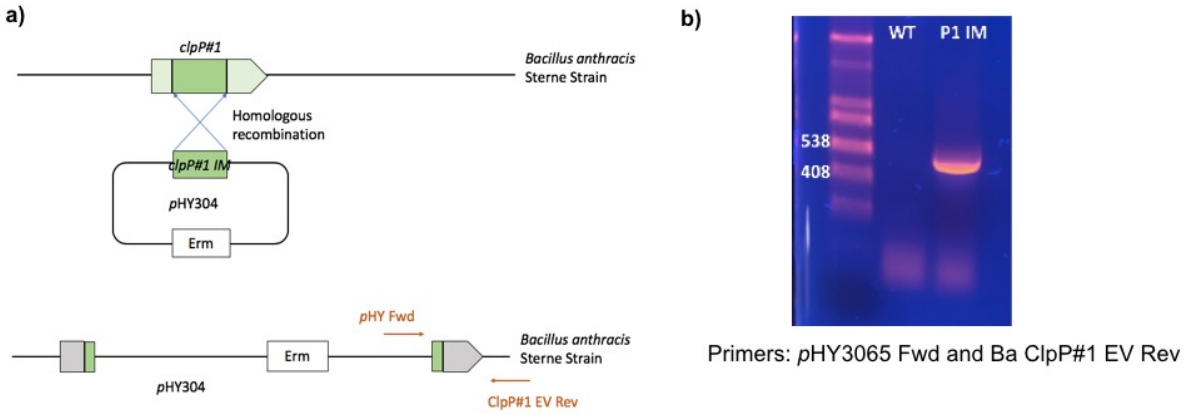

Figure 6. The construction of the *clpP#1* insertional mutant.
a) The *clpP#1* gene is disrupted by integrating a plasmid with the antibiotic resistance gene erythromycin. b) Gel electrophoresis confirmation of plasmid insertion into *B. anthracis* chromosome using pHY3065 Fwd and *B. anthracis* ClpP#1 EV Rev primers.

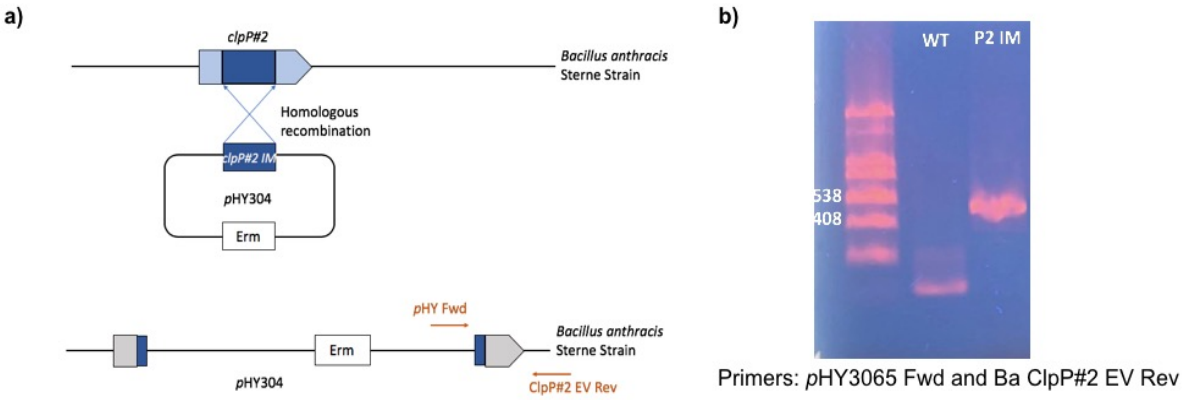

Figure 7. The construction of the *clpP#2* insertional mutant.
a) The *clpP#2* gene is disrupted by integrating a plasmid with the antibiotic resistance gene erythromycin. b) Gel electrophoresis confirmation of plasmid insertion into *B. anthracis* chromosome using pHY3065 Fwd and *B. anthracis* ClpP#2 EV Rev primers.

hour. There were no differences in growth among all four strains in media without antimicrobial agents, suggesting that the media we used had no effects on bacterial growth by itself. To determine the effects of losing each ClpP subunit in the protease on antimicrobial susceptibility, we performed MIC assays using two antimicrobial peptides, LL-37 and nisin, and three antibiotics, penicillin, vancomycin and daptomycin. All of these chemical compounds target the

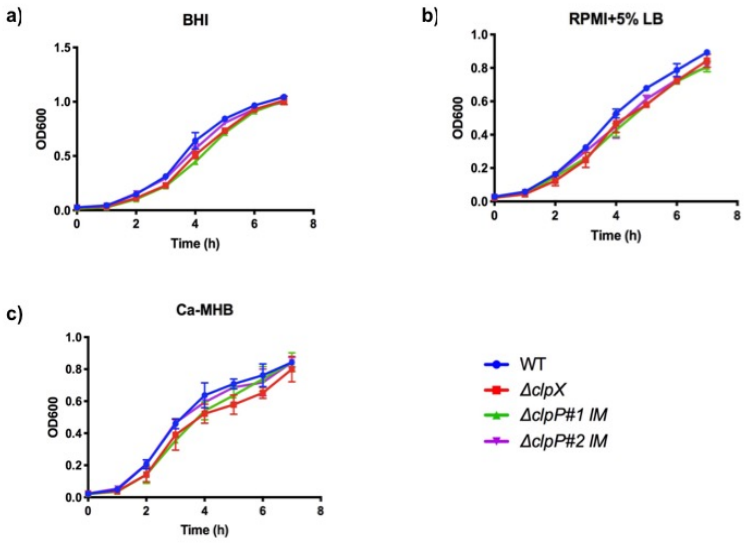

Figure 8. No difference in growth among *B. anthracis* strains in plain media.
Wild-type *B. anthracis* Sterne, Δ*clpX,* Δ*clpP#1* insertional mutant and Δ*clpP#2* insertional mutant were grown in a) BHI, b) RPMI+5%LB and c) CA-MHB. The absorbance was measured every hour for 7 hours. Data is presented as mean+/- SD and the experiment was repeated 2 independent times.

cell envelope, either by targeting the cell wall (penicillin, vancomycin, nisin) or cell membrane (daptomycin, nisin, LL-37). As expected, there was a significant difference in growth between the wild-type *B. anthracis* and Δ*clpX* strain treated by all antibiotics and antimicrobial peptides (Fig. 9b-f). We found inhibition of growth in both the *clpP* insertional mutant strains compared to wild-type Sterne strain for all antibiotics (Fig. 9b-d) and the antimicrobial peptide, nisin (Fig. 9e), but not LL-37 (Fig. 9e). However, neither of the *clpP* mutants had as strong a phenotype as the Δ*clpX*. For example, at 4 μg/ml, daptomycin completely inhibited the growth of Δ*clpX* but the Δ*clpP#1* and Δ*clpP#2* insertional mutants were not inhibited until a concentration of 8 μg/ml (Fig. 9c). The two *clpP* mutants responded to antibiotic treatment in a similar manner for all antibiotics except for penicillin where we have found a small but statistically significant difference between the two *clpP* mutants when treated with penicillin at concentration of 2.5 μg/ml but not at 5 μg/ml (Fig 9b). Therefore, we conclude that both ClpP subunits are both important in antibiotic resistance but the loss of neither individual *clpP* gene alone is as severe as the loss of clpX.

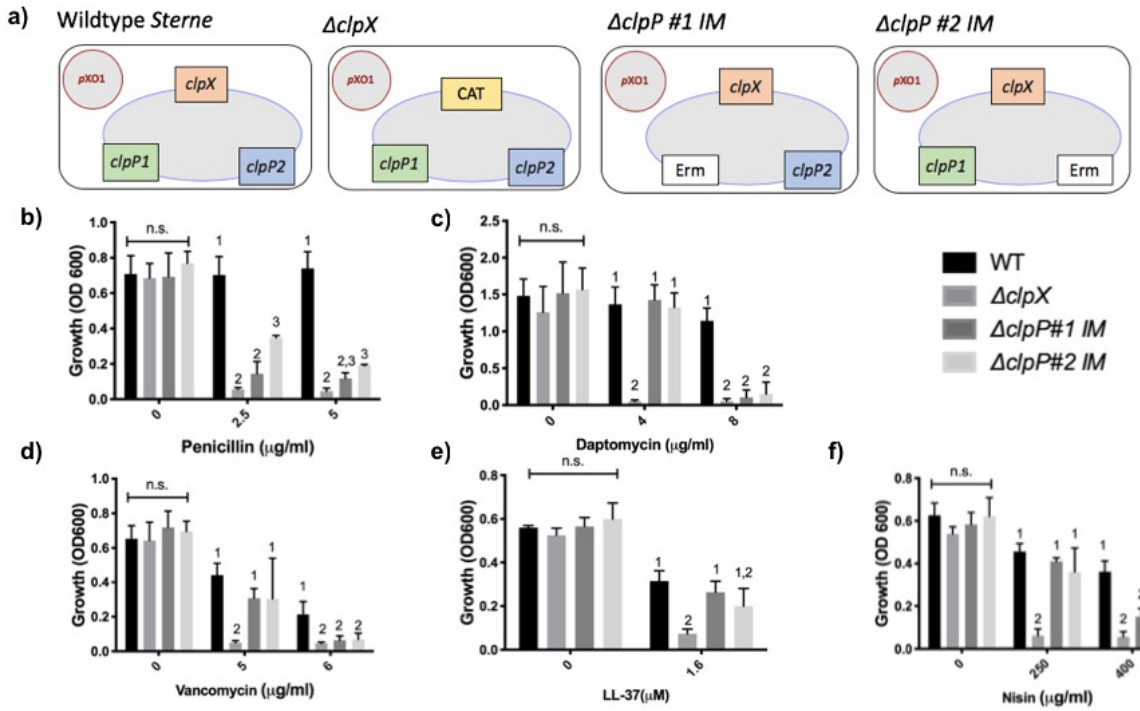

Figure 9. Loss of ClpP#1 and ClpP#2 results in increased antimicrobial susceptibility to cell envelope-targeting antibiotics.
a) Schematic of the 4 bacterial strains: wild-type *B. anthracis* Sterne, Δ*clpX* mutant, Δ*clpP#1* insertional mutant, and Δ*clpP#2* insertional mutant strains. b-f) Growth of wild-type parental *B. anthracis* Sterne (WT), the isogenic Δ*clpX* mutant, the insertional mutant Δ*clpP#1*, insertional mutant Δ*clpP#2* in media containing either (b) penicillin, (c) daptomycin (d) vancomycin, (e) LL-37 or f) nisin at the indicated concentrations. Data is presented as mean+/- SD and assays were repeated at least 3 independent times. Different numbers represent statistical significant groups as $P<0.05$, and n.s. means no statistical difference between groups determined by one-way ANOVA followed by Tukey–Kramer post hoc analysis.

Since we have found that neither *clpP* mutant showed as strong of antibiotic susceptibility as Δ*clpX*, we hypothesized that the ClpP subunits can partially compensate for each other and that loss of both *clpP*1 and *clpP2* genes would be needed to phenocopy loss of *clpX*. To test this, we attempted to construct a double knockout strain with both *clpP#1* and *clpP#2* genes disrupted. We amplified the *clpP#2* gene and sub-cloned into another temperature sensitive plasmid, *p*HY304 with the antibiotic resistant gene kanamycin (*p*HY-Kan) instead of the original plasmid to specifically select for the bacterial colonies containing the mutagenesis plasmid. We successfully transformed the mutagenesis plasmid into the methylation deficient

cells, GM2163, but despite multiple attempts, we could not transform the ClpP#2 IM targeting construct into Δ*clpP#1 B. anthracis*. Therefore were unable to make the double knockout to test this hypothesis.

The ClpXP protease is a global regulator and the loss of either ClpX or ClpP could have effects on *B. anthracis* besides altering cell envelope morphology. Therefore we also tested the *clpP* insertional mutants with four non-cell envelope-targeting antibiotics. Erythromycin, chloramphenicol and tetracycline target the ribosome to inhibit protein biosynthesis, ciprofloxacin targets DNA gyrase to block DNA synthesis. We found no difference among all four *B. anthracis* strains with ciprofloxacin treatment (Fig. 10a) and the disruption of *clpX*

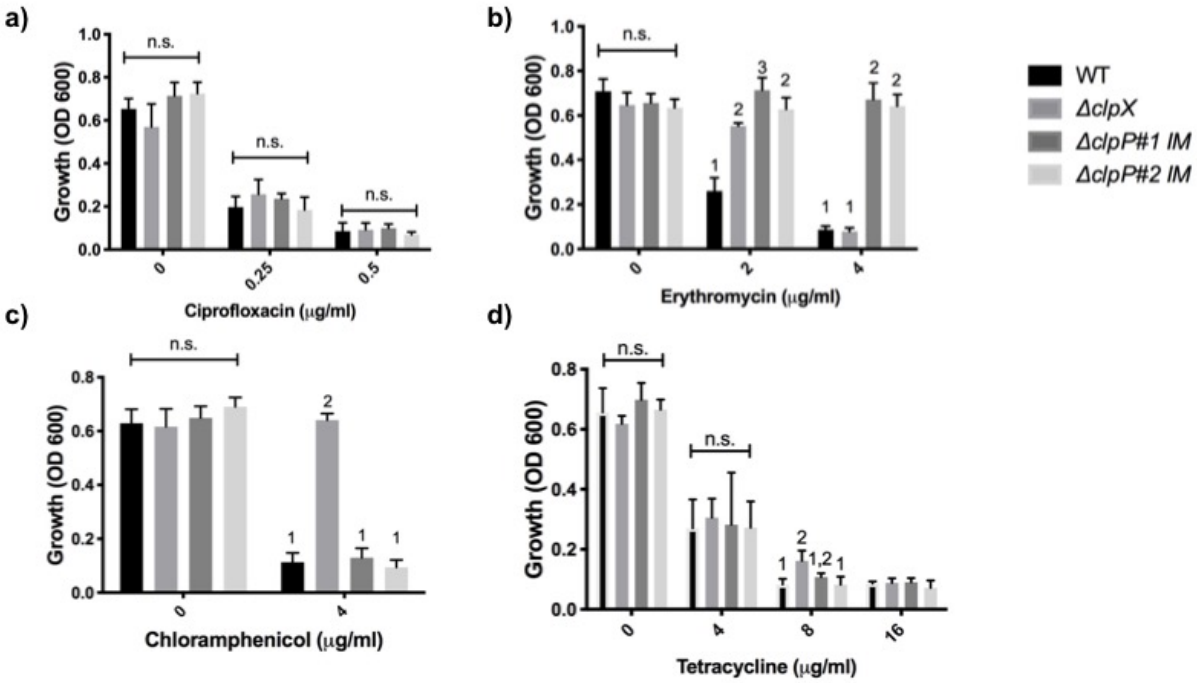

Figure 10. Loss of ClpP#1 and ClpP#2 changes antimicrobial susceptibility to some non-cell envelope-targeting antibiotics.
Growth of wild-type parental *B. anthracis* Sterne (WT), the isogenic Δ*clpX* mutant, the insertional mutant Δ*clpP#1*, and the insertional mutant Δ*clpP#2* in media containing either a) ciprofloxacin, b) tetracycline c) chloramphenicol or d) erythromycin at the indicated concentrations. Data is presented as mean+/- SD and assays were repeated at least 3 independent times. Different numbers represent statistical significant groups as $P<0.05$, and n.s. means no statistical difference between groups determined by one-way ANOVA followed by Tukey–Kramer post hoc analysis.

increases the resistance to tetracycline only very slightly compared to wild-type and Δ*clpP#2* strains (Fig. 10b). Surprisingly, there were notable differences with the other two antibiotics. The loss of *clpX* actually increased resistance to chloramphenicol although neither *clpP* insertional mutants showed any changes in susceptibility relative to wild-type (Fig. 10c). We saw the opposite result with erythromycin, where both the *clpP* insertional mutants showed increased resistance while Δ*clpX* was unaffected (Fig. 10d).

Complementation of *clpP* insertional mutant in *B. anthracis*

Since the insertional mutation in ClpP subunits increases the susceptibility to cell envelope-targeting antibiotics, we created complemented strains for both Δ*clpP#1* and Δ*clpP#2* to make sure all the phenotypes were caused by the loss of function of *clpP*s rather than an unintended mutation. The *clpP#1* gene and *clpP#2* gene in *B. anthracis* Sterne strain were amplified and inserted into the same inducible expression plasmid *p*UTE657 (Fig. 11a, 11c) that was used previously to complement Δ*clpX*. The *clpP#1* and *clpP#2* complement plasmids were transformed into *B. anthracis* Δ*clpP#1* and *B. anthracis* Δ*clpP#2* insertional mutants respectively. To confirm the successful insertion, the primers specific to *p*UTE657 were used to amplify the insertion site of the plasmid, generating a band size of about 800bp for both Δ*clpP* complement strains (Fig. 11b, 11d). For the control of the plasmid, the empty vector *p*UTE657 was also transformed into wild-type *B. anthracis*, Δ*clpP#1* and Δ*clpP#2* insertional mutant strains (not shown). The same primers were used to confirm the transformation, forming a 276bp band (Fig. 11b, 11d). This created strains: Δ*clpP#1*+ *p*UTE657 and Δ*clpP#1*+ *pclpP#1* (Fig. 12a), and Δ*clpP#2*+ *p*UTE657 and Δ*clpP#2* + *pclpP#2* (Fig. 13a).

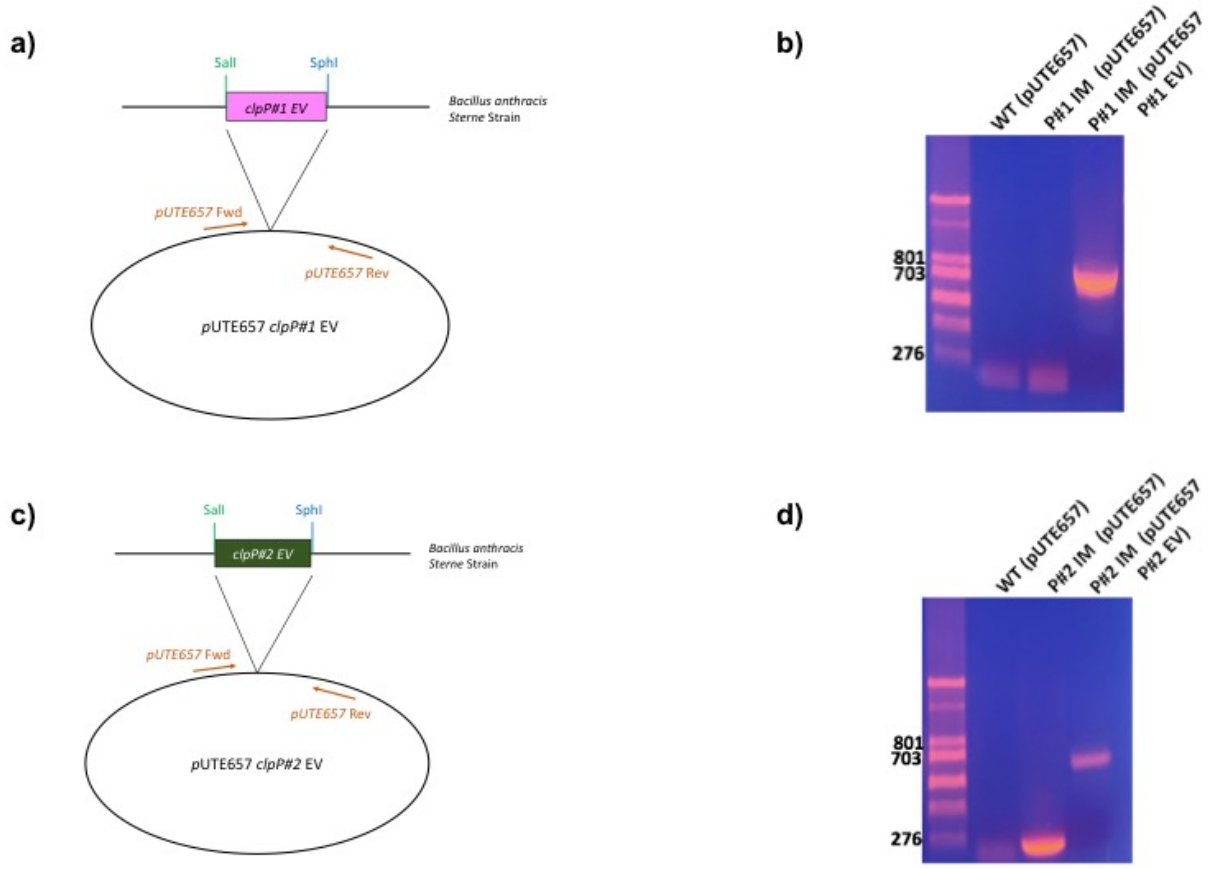

Figure 11. The construction of *clpP#1* and *clpP#2* expression plasmids for complementation. Diagrams of the *clpP*#1 (a) or *clpP*#2 (c) genes sub-cloned into the inducible plasmid *p*UTE657 b, d) Gel electrophoresis confirmation of successful sub-cloning using *p*UTE657 Fwd and *p*UTE657 Rev primers.

ClpP is essential for *B. anthracis* resistance to cell envelope-targeting antibiotics

To determine the effects of disrupting the function of each ClpP subunit on antimicrobial susceptibility, we performed MIC assays using penicillin, daptomycin, and LL-37. All these compounds target the bacterial cell envelope. All the antibiotics and antimicrobial peptides showed a significant difference in growth inhibition between the wild-type *B. anthracis* and either Δ*clpP#1*+*p*UTE657 (Fig. 12b-d) and Δ*clpP#2* +*p*UTE657 (Fig. 13b-d) strains. There was no significant difference between wild-type and complemented strains. Therefore, we conclude that these phenotypes are not due to an unintended mutation and the *clpP#1* and *clpP#2* genes are necessary for antibiotic resistance against antibiotics that target the cell envelope.

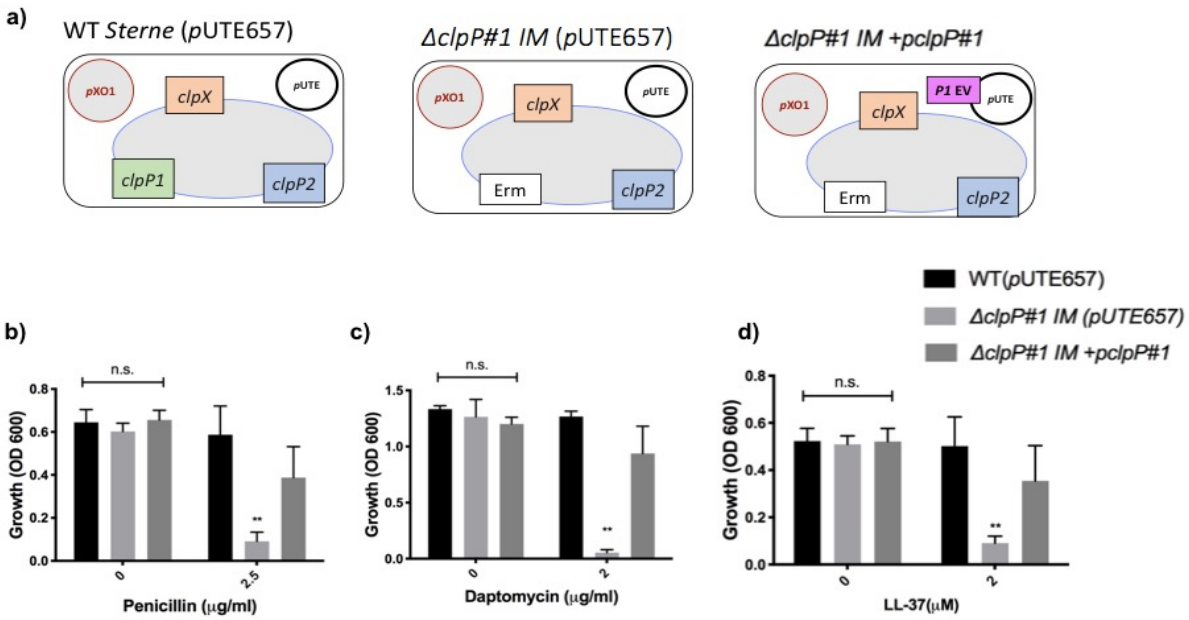

Figure 12. The presence of ClpP#1 subunit is necessary for decreased antimicrobial susceptibility in *B. anthracis*.

a) Schematic of the 3 bacterial strains: wild-type parental *B. anthracis* Sterne carrying the empty inducible plasmid *p*UTE657 used for all complementation assays (WT+*p*UTE657), the insertional mutant Δ*clpP#1* containing empty *p*UTE657 (Δ*clpP#1*+*p*UTE657), and the Δ*clpP#1* insertional mutant containing the wild-type *clpP#1* gene in *p*UTE657 (*ΔclpP#1* + *pclpP#1*). b-d) Growth of WT + *p*UTE657, Δ*clpP#1* + *p*UTE657 and Δ*clpP#1* + *pclpP#1* in media containing either (b) penicillin, (c) daptomycin or (d) LL-37 at the indicated concentrations. Data is presented as mean+/- SD and assays were repeated at least 3 independent times. Statistically significant differences from wild-type growth are represented by *P<0.05, **P<0.01, and n.s. means no statistical difference between two groups determined by one-way ANOVA followed by Tukey–Kramer post hoc analysis.

Verification of virulence in *B. anthracis* mutants in *G. mellonella* infection model

To determine the effects of disrupting ClpP subunits in animal survival, we used the waxworm *Galleria mellonella*, which is considered a reliable *in vivo* model for *B. anthracis* infection studies because it is an invertebrate and shares similarities to mammalian immune system (Malmquist et al., 2019). Since the human cathelicidin antimicrobial peptide, LL-37 we used in MIC assay is one of the components in innate immune system, this assay provides connection between antimicrobial susceptibility and virulence. *G. mellonella* has both larval and moth forms, and we separated larvae into treatment groups of 12 weighing 190-220mg each (Fig. 14a) to minimize the effects caused by difference in weight. The bacterial cultures were grown

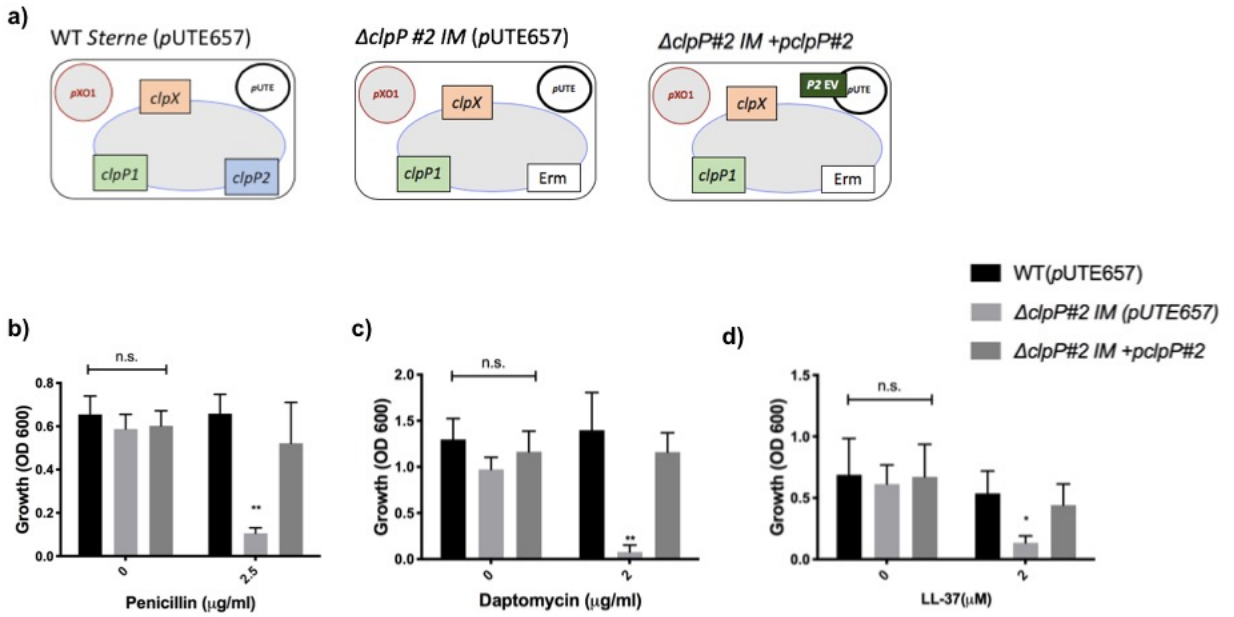

Figure 13. The presence of ClpP#2 subunit is necessary for increased antimicrobial susceptibility in *B. anthracis*.

a) Schematic of the 3 bacterial strains: wild-type parental *B. anthracis* Sterne carrying the empty inducible plasmid *p*UTE657 used for all complementation assays (WT+*p*UTE657), the insertional mutant Δ*clpP2* containing empty *p*UTE657 (Δ*clpP#2*+*p*UTE657), the Δ*clpP#2* insertional mutant containing the wild-type *clpP#2* gene in *p*UTE657 (*ΔclpP#2* + *pclpP#2*). b-d) Growth of WT + *p*UTE657, Δ*clpP#2* + *p*UTE657 and Δ*clpP#2* + p*clpP*#2 in media containing either (b) penicillin, (c) daptomycin or (d) LL-37 at the indicated concentrations. Data is presented as mean+/- SD and assays were repeated at least 3 independent times. Statistically significant differences from wild-type growth are represented by *P<0.05, **P<0.01, and n.s. means no statistical difference between two groups determined by one-way ANOVA followed by Tukey–Kramer post hoc analysis.

into early log phase, washed and diluted 1:2 in PBS for injection. The number of dead larva was easy to distinguish because the larva turned black after death (Fig. 14b, white arrows) and larval survival was assessed every 24 hours until 72 hours. As expected, the larval group injected with PBS showed a high survival rate while the group with injected with wild-type Sterne *B. anthracis* had the highest mortality (over 50% mortality rate after 72 hour incubation) (Fig. 14c). The group with the Δ*clpX* strain injection also had a high survival rate (Fig. 14c). Neither Δ*clpP#1* and Δ*clpP#2* injected larvae showed significant difference in survival rate from wild-type Sterne *B. anthracis* group. The larval group with Δ*clpP#1* injection showed difference in growth from Δ*clpX* group, but the group with Δ*clpP#2* injection did not. We also did not find

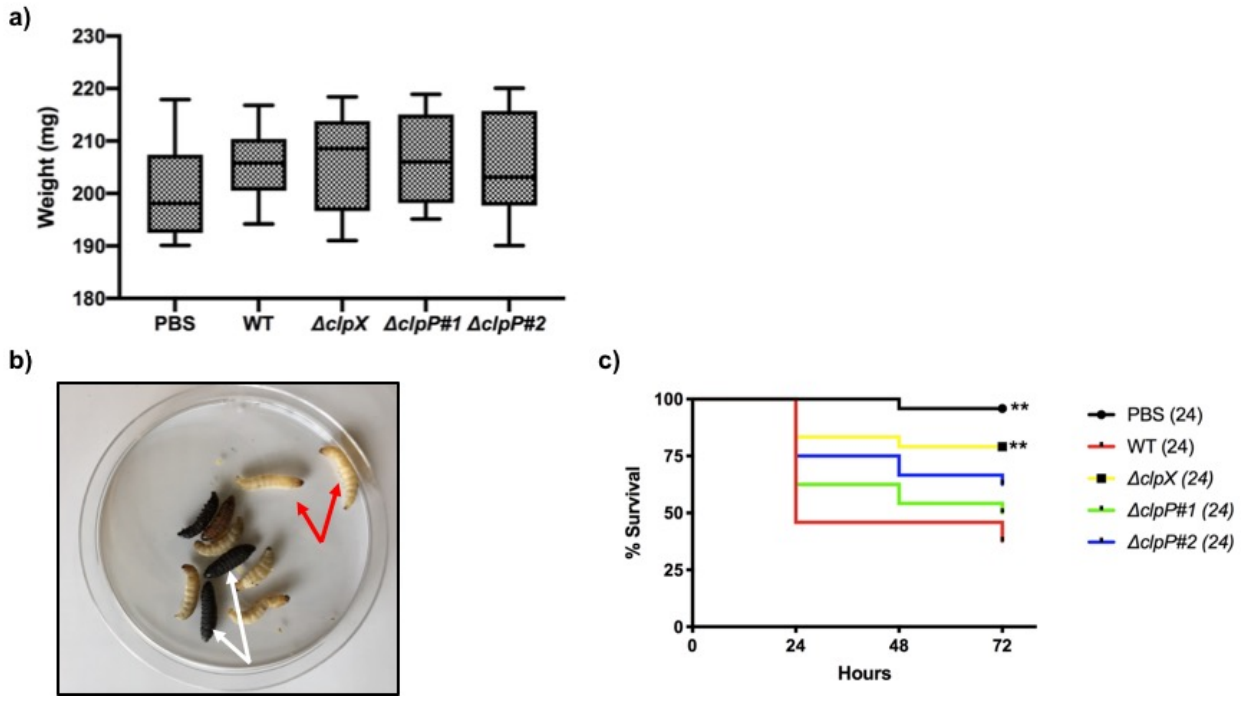

Figure 14. *B. anthracis clpP#1* and *clpP#2* mutant strains do not have attenuated virulence in *G. mellonella*

a) Larval weights for each injection group. b) Representative figure of infected *G. mellonella* with dead larvae (white arrow) and living larvae (red arrow). c) Percent survival of larvae injected with saline (PBS), wild-type *B. anthracis* Sterne (WT), Δ*clpP#1* insertional mutant, and Δ*clpP#2* insertional mutant at 24, 48, and 72 hours. Each infection was repeated two independent times with 12 larvae per condition and total number of worms for each condition are shown in parantheses. Statistical significance from larva injected with wild-type Sterne strain are represented by *P<0.05, **P<0.01, as determined by Log-rank test.

any difference between the two Δ*clpP* injection groups. Therefore, we conclude that loss of either gene alone does not seem to have any effects on virulence.

Discussion

One of our major goals was to identify whether the ClpX-mediated antibiotic resistance is ClpP dependent. To do this, we created the substitution mutation at the ClpX-ClpP interaction site and found that inhibition of the ClpXP protease formation in *B. anthracis* resulted in the increased susceptibility to cell envelope-targeting antibiotics and changed cellular morphology, the same phenotypes as the loss of *clpX*. Therefore, we conclude that ClpX interacts with ClpP as a protease when mediating resistance to cell-envelope targeting antibiotics. It is less clear what

the mechanism of antibiotic resistance is although there may be a relationship between resistance and cell envelope characteristics. Previous research in our lab has found differences in cellular morphology in Δ*clpX* including a decrease in cell wall thickness and the cell division defects when incubated in RPMI+ 5% LB (Evans, unpublished data). We wanted to determine whether the inhibition of protease formation leads to similar cell morphology changes as Δ*clpX*. To accomplish this, we performed a buoyancy assay, hydrophobicity assay and used scanning electron microscopy to look at the cell surface. We used a buoyancy assay because this measures cell density and cell wall thickness is related to cell density. Increased cell wall thickness has previously been linked to antibiotic resistance (Mishra et al., 2011). However, the buoyancy assay is an indirect measure of cell wall thickness because it is not the only factor in cell density (Makinoshima et al., 2002). However, our results do correlate with those of a previous graduate student who showed decreased cell wall thickness in Δ*clpX* using TEM and it lends support to the hypothesis that this change is dependent on ClpXP protease inhibition. Surface hydrophobicity is also known to relate to antibiotic resistance. One study on *S. aureus* found a higher surface hydrophobicity in the resistant strain compared to the wild-type (Lather et al., 2016). This finding is opposite from our results. We found that the loss of the *clpX* gene and the inhibition of protease formation increases the cell surface hydrophobicity; however, we expected to have a more hydrophilic cell surface in both Δ*clpX* and Δ*clpX*+*pclpX*^{I265E} mutants based on the findings in *S. aureus*. The results indicated that the surface hydrophobicity plays some role in antibiotic susceptibility in Δ*clpX* and Δ*clpX*+*pclpX*^{I265E} mutants, but the specific relationship between the two is unknown. Lastly, we also looked at cell division defects using scanning electron microscopy. Although the SEM images we obtained lend support to improper cell division, as was seen by our previous graduate student (Evans, unpublished data), these defects

were not common in our images. It is likely that inappropriate cell division could be occurring more frequently than can be seen in scanning electron microscopy, which only shows surface images. A more detailed analysis of division sites would require images generated via transmission electron microscopy. Taken together, our data further support the finding that changes in cell envelope morphology occur with the loss of *clpX* and inhibition of protease formation.

After clarifying the role of ClpX as a protease in antibiotic resistance and morphological changes, we wanted to determine the function of the two ClpP subunits in *B. anthracis* as well. We found that the disruption of either the *clpP#1* or *clpP#2* gene leads to increased susceptibility to cell envelope-targeting antibiotics. Both *clpP* mutants were more susceptible to all cell-envelope active antibiotics and these phenotypes were complemented with an expression plasmid carrying the disrupted *clpP* gene. Neither Δ*clpP#1* nor Δ*clpP#2* are as susceptible as Δ*clpX* to cell envelope-targeting antibiotics, suggesting that while both the ClpP subunits play a role in antibiotic resistance, they can partially compensate for each other. One strange result was that while Δ*clpP#1* and Δ*clpP#2* carrying the empty plasmid *p*UTE657 used in the complementation assays showed increased susceptibility to LL-37 (Fig. 12d, 13d), no difference was seen when we compared the susceptibility of Δ*clpX*, Δ*clpP#1* and Δ*clpP#2* without empty vector (Fig. 9e). Different concentrations of LL-37 were used in these figures, so it is possible that is accounting for the different results. It is also possible that the empty vector *p*UTE657 is affecting resistance. Further experiments will be needed to resolve this discrepancy.

When treated with non-cell envelope-targeting antibiotics, the resistance pattern differed between the bacterial strains and the antibiotics. No differences in susceptibility between wild-type and the two *clpP* mutants were seen for ciprofloxacin, tetracycline or chloramphenicol,

however, the two *clpP* mutants were much more resistant to erythromycin and Δ*clpX* was much more resistant to chloramphenicol than even the wild-type strain (Fig. 10). Both erythromycin and chloramphenicol target the 23S rRNA of the 50S ribosomal subunit, but chloramphenicol binds to the A2451 and A2452 residues specifically. Tetracycline targets the 30S ribosomal subunit, and ciprofloxacin binds to the DNA gyrase. Based on their mechanism of action, there is no obvious explanation for these observations. However, it is likely that loss of *clpX* or *clpP* are changing the overall stress response to antibiotic treatment and could account for the changes in overall resistance. Additional studies are needed to better understand the role the ClpXP protease and its individual subunits are playing in overall antibiotic resistance.

We also tested the virulence of the *clpP* mutant strains *in vivo* using a *G. mellonella* infection model. We did not observe any significant difference in survival between wild-type and the two *clpP* mutant injected groups. However, we were only able to perform the survival assay two independent times, rather than three as originally planned due to the campus shutdown. It is possible there are survival differences, particularly between the wild-type and Δ*clp#2* mutant which has a p-value is 0.08. Another option to assess virulence is to use a competition model of virulence, which is a more sensitive assay than the survival model (Malmquist et al., 2019). In the competition model, we would inject one worm with both wild-type and one of the *clpP* mutant strains for direct growth competition. If there is virulence attenuation in the *clpP* mutant, the wild-type bacteria will proliferate more in the model. Regardless, we are not surprised that the *clpP* mutants do not have as strong of a virulence phenotype as the Δ*clpX* mutant as we see similar results in our antibiotic assays. The loss of *clpX* results in a more attenuated bacterium than loss of either single *clpP* gene.

It is very rare for gram-positive bacteria to have two ClpP subunits. The acid-fast stained *Mycobacterium tuberculosis* and gram-negative *Pseudomonas aeruginosa* are two examples of bacteria known to have two ClpP subunits, considered relevant to the protease structure in *B. anthracis*. Studies on *M. tuberculosis* have found that the proteolytic activity decreased in both *clpP#2* mutant strain and *clpP* double-knockout strain, suggesting that subunit ClpP#2 is important for proteolysis as well as the ClpX-mediated protease function (Nagpal et al., 2019). The relative non-essential subunit, ClpP#1 in *M. tuberculosis* is required for the construction of a double-ring ClpP#1P#2 complex (Nagpal et al., 2019). The ClpP#1 does not contribute to protein regulation, but it can start pro-peptide processing, known as protein cleavage only when ClpP#1 subunit is presented independently of regulatory ATPase (Nagpal et al., 2019). Another study on *P. aeruginosa* has discovered that the purified ClpP#1 or both purified ClpP subunits showed repression in ATP hydrolysis, suggesting that the ClpP#1 subunit is essential for ClpXP protease function in *P. aeruginosa*, while the ClpP#2 is required for upstream microcolony organization of the chronic lung disease (Hall et al., 2017). The role of the two ClpPs subunits differ more in *M. tuberculosis* and *P. aeruginosa* compared to what we found in *B. anthracis*. Since *B. anthracis* is not closely related to the other two bacteria and the two subunits in *B. anthracis* have higher similarity in protein sequence, it is not surprising to find a similar role for the *clpP#1* and *clpP#2* genes, at least in antibiotic resistance.

Our findings validated the interaction between ClpX-ClpP in antibiotic resistance and morphological changes and determined that both ClpP subunits are important for resistant to cell envelope antibiotics in *B. anthracis* Sterne. However, neither mutant showed as strong of a phenotype as the loss of just *clpX*. This is likely because the two ClpPs can partially compensate to each other. Removal of both *clpP* genes would likely have a stronger effect and is more likely

to have the same phenotype as Δ*clpX*. Unfortunately, due to technical problems, we could not create the *clpP#1* and *clpP#2* double-knockout to test this hypothesis. ClpP has been proposed as a drug target since the deficiency of ClpP impairs virulence *in vivo* (Raju et al., 2012; Zhao et al., 2016). The drug, acyldepsipeptides, specifically targets ClpP subunit to induce uncontrolled proteolytic activity, leading to inhibition of cell division and cell death (Brötz-Oesterhelt et al., 2005). Our results demonstrate that while ClpP could be an effective drug target in *B. anthracis*, both subunits would likely need to be targeted for a maximum effect. However, targeting the ClpXP protease would significantly impair *B. anthracis* function. Therefore, studying the role of ClpP subunits together with ClpX has helped us better understand the mechanisms and factors contributing to antibiotic resistance and virulence in *B. anthracis*.

REFERENCES

Agrawal, A. & Pulendran, B. (2004). Anthrax lethal toxin: a weapon of multisystem destruction. *CMLS, Cell. Mol. Life Sci. 61*(22): 2859-2865.

Baillie, L., and Read, T.D. (2001). *Bacillus anthracis*, a bug with attitude!. *Curr Opin Microbiol. 4*(78), 81.

Baker, T.A.,& Sauer, R.T. (2012). ClpXP, an ATP-powered unfolding and protein degradation machine. *Biochim Biophys Acta. 1823*(1), 15-28.

Brötz-Oesterhelt H, Beyer D, Kroll HP, Endermann R, Ladel C, Schroeder W, Hinzen B, Raddatz S, Paulsen H, Henninger K, Bandow JE, Sahl HG, Labischinski H. (2005). Dysregulation of bacterial proteolytic machinery by a new class of antibiotics. *Nat Med 11*(10), 1082-7

Claunch K.M., Bush M., Evans C.R., Malmquist J.A., Hale M.C. McGillivray S.M. (2018). Transcriptional profiling of the clpX mutant in Bacillus anthracis reveals regulatory connection with the lrgAB operon. *Microbiology Society Journal 164*(4), 659-669

Dixon, T. C., Meselson, M., Guillemin, J., & Hanna, P. C. (1999). Anthrax. *New England Journal of Medicine 341*(11), 815-826.

Evans, R.C. (unpublished). Investigation of the ClpXP protease's connection to *Bacillus anthracis* cell wall characteristics. Texas Chrsitian University, Fort Worth, Texas.

Fedhila, S., Msadek, T., Nel, P., & Lereclus, D. (2002). Distinct clpP genes control specific adaptive responses in *Bacillus thuringiensis*. *Journal of bacteriology 184*(20), 5554-5562.

Frees, D., Savijoki, K., Varmanen, P., and Ingmer, H. (2007). Clp ATPases and ClpP Proteolytic complexes regulate vital biological processes in low GC, Gram-positive bacteria. *Mol Microbiol. 63*(1285),295.

George Sitterley. (2008). Attachment and matrix factors. *Sigma Life Science BioFiles 3*(8), 12

Hall, B. M., Breidenstein, E., de la Fuente-Núñez, C., Reffuveille, F., Mawla, G. D., Hancock, R., & Baker, T. A. (2017). Two Isoforms of Clp Peptidase in *Pseudomonas aeruginosa* Control Distinct Aspects of Cellular Physiology. *Journal of bacteriology 199*(3), e00568 -16.

Hanaki, H., Kuwahara A.K., Boyle V.S., Daum, R.S., Labischinski, H., and Hiramatsu, K. (1998). Activated cell wall synthesis is associated with vancomycin resistance in methicillin resistant *Staphylococcus aureus* clinical strains Mu3 and Mu50. *Journal of Antimicrobial Chemotherapy 42*, 199-209.

Harris SH. (1994). Factories of death: Japanese secret biological warfare, 1932- 1945, and the American cover-up. London: Routledge.

Hart, C.A., and Beeching, N.J. (2002). A spotlight on anthrax. *Clin Dermatol. 20*(365), 375.

Jernigan, D. B., Raghunathan, P. L., Bell, B. P., Brechner, R., Bresnitz, E. A., Butler, J. C., …Gerberding, J.L. (2002). Investigation of bioterrorism-related anthrax, United States, 2001: epidemiologic findings. *Emerging Infect. Dis, 8*(10), 1019-1028.

Lather, P., Mohanty, A. K., Jha, P., & Garsa, A. K. (2016). Contribution of Cell Surface Hydrophobicity in the Resistance of *Staphylococcus aureus* against Antimicrobial Agents. *Biochemistry research international 2016*: 1091290.

Makinoshima H., Nishimura A., Ishihama A. (2002). Fractionation of *Escherichia coli* cell populations at difference stages during growth transition to stationary phase. *Mol Microbiol 43*(2): 269-79

Malmquist J.A., Rogan M.R. McGillivray S.M. (2019). *Galleria mellonella* as an infection model for *Bacillus anthracis* Sterne. *Front. Cell. Infect. Microbiol. 9*, 360

McGillivray S.M., D. N. T., Nitya S. Ramadoss, John N. Alumasa, Cheryl Y. Okumura, George Sakoulas, Micah M. Vaughn, Dawn X. Zhang, Kenneth C. Keiler, Victor Nizet. (2012). Pharmacological Inhibition of the ClpXP Protease Increases Bacterial Susceptibility to Host Cathelicidin Antimicrobial Peptides and Cell Envelope-Active Antibiotics. *Antimicrobial Agents and Chemotherapy 56*(4):1854-61

McGillivray S.M., E. C. M., Fisher N., Sabet M. · Zhang D.X., Chen Y., Haste N.M., Aroian R.V., Gallo R.L., Guiney D.G., Friedlander A.M., Koehler T.M., Nizet V. (2009). ClpX Contributes to Innate Defense Peptide Resistance and Virulence Phenotypes of *Bacillus anthracis*. *Journal of Innate Immunity 1*, 494–506.

Mishra, N.N., McKinnell, J., Yeaman, M.R., Rubio, A., Nast, C.C., Chen, L., Kreiswirth, B.N., and Bayer, A.S. (2011). In vitro cross resistance to daptomycin and host defense cationic antimicrobial peptides in clinical methicillin resistant *Staphylococcus aureus* isolates. *Antimicrob Agents Chemother. 55*, 4012-18.

Muthaiyan A, Silverman JA, Jayaswal RK, Wilkinson BJ. (2008). Transcriptional profiling reveals that daptomycin induces the *Staphylococcus aureus* cell wall stress stimulon and genes responsive to membrane depolarization. *Antimicrob. Agents Chemother. 52*:980 -990.

Nagpal, J., Paxman, J. J., Zammit, J. E., Alhuwaider, A., Truscott, K. N., Heras, B., & Dougan, D. A. (2019). Molecular and structural insights into an asymmetric proteolytic complex (ClpP1P2) from *Mycobacterium smegmatis*. *Scientific reports 9*(1), 18019.

Nikolaidis, I., Favini-Stabile, S., & Dessen, A. (2014). Resistance to antibiotics targeted to the bacterial cell wall. *Protein science : a publication of the Protein Society 23*(3), 243–259.

Raju RM, Unnikrishnan M, Rubin DHF, Krishnamoorthy V, Kandror O, et al. (2012). *Mycobacterium tuberculosis* ClpP1 and ClpP2 Function Together in Protein Degradation and Are Required for Viability *in vitro* and During Infection. *PLOS Pathogens 8*(2): e1002511.

Read, T. D., Peterson, S. N., Tourasse, N., Baillie, L. W., & al, e. (2003). The genome sequence of *Bacillus anthracis* Ames and comparison to closely related bacteria. *Nature 423*(6935), 81-6.

Singh Y, Leppla SH, Bhatnagar R, Friedlander AM. (1989). Internalization and processing of *Bacillus anthracis* lethal toxin by toxin-sensitive and -resistant cells. *J Biol Chem. 264*(19): 11099–11102.

Stahlhut S.G., Alqarzaee A.A., Jensen C., Fisker N.S., Pereira A.R. (2017). The ClpXP protease is dispensable for degradation of unfolded proteins in *Staphylococcus aureus*. *Scientific Reports 7*, 11739

Thwaite JE, Hibbs S, Titball RW, Atkins TP. (2006). Proteolytic degradation of human antimicrobial peptide LL-37 by *Bacillus anthracis* may contribute to virulence. *Antimicrob Agents Chemother 50*:2316–2322.

Watson, A., & Keir, D. (1994). Information on Which to Base Assessments of Risk from Environments Contaminated with Anthrax Spores. *Epidemiology and Infection 113*(3), 479-490.

Wawrzynow, A., Wojtkowiak, D., Marszalek, J., Banecki, B., Jonsen, M., Graves, B., Georgopoulos, C., & Zylicz, M. (1995). The ClpX heat-shock protein of *Escherichia coli*, the ATP-dependent substrate specificity component of the ClpP-ClpX protease, is a novel molecular chaperone. *The EMBO journal 14*(9), 1867–1877.

Zhao, B. B., Li, X. H., Zeng, Y. L., & Lu, Y. J. (2016). ClpP-deletion impairs the virulence of *Legionella pneumophila* and the optimal translocation of effector proteins. *BMC microbiology 16*(1), 174.

Lang Zou

Education	M.S. Biology, Texas Christian University, Fort Worth, TX (2020) B.S. Biology, University of Washington, Seattle, WA (2018)
Teaching Experience	Graduate Teaching Assistant, BIOL 10501/10511 Introductory Biology Labs, 2018-20
Funding	Adkins Fellowship, Department of Biology, TCU (2019) Graduate Teaching Assistantship, Department of Biology, TCU (2018-20) TCU Science and Engineering Research Center Grant (2019-20)

ABSTRACT

INVASTIGATING THE ROLE OF CLPP- AND CLPX-MEDIATED ANTIMICROBIAL RESISTANCE IN *BACILLUS ANTHRACIS*

By Lang Zou, M.S. 2020

Department of Biology

Texas Christian University

Major professor: Dr. Shauna M. McGillivray, Associate Professor of Biology

The regulatory ATPase ClpX in *Bacillus anthracis* contributes to resistance against cell-wall active antibiotics. ClpX can function independently as a chaperone or together with ClpP to form the ClpXP protease. It is unclear whether ClpX-mediated antibiotic resistance in *B. anthracis* is dependent on ClpP and, if so, which of the two *clpP* genes found in *B. anthracis* is important in antibiotic resistance. To do this, we created a strain of *B. anthracis* Sterne that is unable to form the ClpXP protease and found increased susceptibility to cell envelope-targeting antibiotics, suggesting that ClpX-mediated antibiotic resistance is dependent on ClpP. Then, we constructed insertional mutants in each of the two *clpP* genes, Δ*clpP#1* and Δ*clpP#2*, and found significantly increased susceptibility to cell-envelope active antibiotics in both the *clpP* insertional mutants. However, neither Δ*clpP#1* nor Δ*clpP#2* showed as strong a phenotype as *ΔclpX*, suggesting that the two ClpPs can partially compensate for each other.